Plant Mol Biol (2009) 71:379–390
DOI 10.1007/s11103-009-9529-3

AtObgC, a plant ortholog of bacterial Obg, is a chloroplast-targeting GTPase essential for early embryogenesis

Woo Young Bang · Akira Hata · In Sil Jeong · Tetsuya Umeda · Takayuki Masuda · Ji Chen · Ishizaki Yoko · I Nengah Suwastika · Dae Won Kim · Chak Han Im · Byung Hyun Lee · Yuno Lee · Keun Woo Lee · Takashi Shiina · Jeong Dong Bahk

Received: 6 July 2009 / Accepted: 14 July 2009 / Published online: 28 July 2009

Abstract Obg is a ribosome-associated GTPase essential for bacterial viability and is conserved in most organisms, from bacteria to eukaryotes. Obg is also expressed in plants, which predicts an important role for this molecule in plant viability; however, the functions of the plant Obg homologs have not been reported. Here, we first identified *Arabidopsis* AtObgC as a plant chloroplast-targeting Obg and elucidated its molecular biological and physiological properties. *AtObgC* encodes a plant-specific Obg GTPase that contains an N-terminal region for chloroplast targeting and has intrinsic GTP hydrolysis activity. A targeting assay using a few AtObgC N-terminal truncation mutants revealed that AtObgC localizes to chloroplasts and its transit peptide consists of more than 50 amino acid residues. Interestingly, GFP-fused full-length AtObgC exhibited a punctate staining pattern in chloroplasts of *Arabidopsis* protoplasts, which suggests a dimerization or multimerization of AtObgC. Moreover, its Obg fold was indispensable for the generation of the punctate staining pattern, and thus, was supposed to be important for such oligomerization of AtObgC by mediating the protein–protein interaction. In addition, the T-DNA insertion *AtObgC* null mutant exhibited an embryonic lethal phenotype that disturbed the early stage of embryogenesis. Altogether, our results provide a significant implication that AtObgC as a chloroplast targeting GTPase plays an important role at the early embryogenesis by exerting its function in chloroplast protein synthesis.

Keywords Chloroplast · Embryogenesis · GTPase · Obg · Ribosome

Abbreviations

G domain	GTPase domain
GFP	Green fluorescent protein
OCT	Obg C-terminal region
PPR	Pentatrico-peptide repeat
RFP	Red fluorescent protein

Introduction

GTPase proteins are essential for a variety of basic cellular processes, which include signal transduction, protein synthesis, membrane trafficking, and cell proliferation, and are conserved in almost all organisms, ranging from prokaryotes to eukaryotes (Bourne et al. 1990, 1991; Cabrera-Vera et al. 2003; Caldon and March 2003). GTPases share common properties, form relatively stable complexes with

Woo Young Bang, Akira Hata and In Sil Jeong contributed equally to this work.

Electronic supplementary material The online version of this article (doi:10.1007/s11103-009-9529-3) contains supplementary material, which is available to authorized users.

W. Y. Bang · I. S. Jeong · J. Chen · D. W. Kim · C. H. Im · B. H. Lee · Y. Lee · K. W. Lee · J. D. Bahk (✉)
Division of Applied Life Sciences (BK21 and EB-NCRC), Graduate School of Gyeongsang National University, Jinju 660-701, Korea
e-mail: jdbahk@gnu.ac.kr

A. Hata · T. Umeda · T. Masuda · I. Yoko · T. Shiina
Graduate School of Human and Environmental Sciences, Kyoto Prefectural University, Shimogamo, Sakyo-ku, Kyoto 606-8522, Japan

IN. Suwastika
Graduate School of Biostudies, Kyoto University, Sakyo-ku, Kyoto 606-8502, Japan

GTP and GDP, and hydrolyze GTP (Sprang 1997). Among them, Ras-like small GTPases have been studied widely as molecular switches of downstream events in cellular signaling pathways, by cycling between three states, i.e., a GTP-bound form (active state), a GDP-bound form (inactive state), and an empty form (transient state) (Bar-Sagi and Hall 2000). In addition, this cycle was reported to be regulated by several GTPase effectors, which include GTPase activating protein (GAP), guanine nucleotide release factor (GNRF), GDP dissociation inhibitor (GDI), and GDP/GTP exchange factor (GEF) (Bar-Sagi and Hall 2000; Sprang 1997).

The small GTPases possess a single common structural core, the so-called G domain, which forms the guanine-nucleotide-binding site (Sprang 1997); however, some GTPase protein subfamilies consist of a large peptide that encompasses, in addition to the G domain, other domains of unknown function (Leipe et al. 2002). Moreover, many studies have reported that the large GTPases play important roles in many aspects of various biological processes (Brown 2005; Caldon and March 2003; Czyz and Wegrzyn 2005; Leipe et al. 2002). Particularly, the Obg subfamily of GTPases are the object of recent interest, as their demonstrated importance for bacterial viability may represent a potential target for the development of new antibacterial drugs (Comartin and Brown 2006). The *Obg* gene, which encodes the SpoOB-associated GTP-binding protein, was originally identified downstream of the *SpoOB* gene in *Bacillus subtilis* (Trach and Hoch 1989) and the study of its structure revealed that typical Obgs are large GTPases composed of three domains, i.e., the Obg fold, the G domain, and the OCT, an Obg C-terminal region (Buglino et al. 2002; Kukimoto-Niino et al. 2004). Despite the widespread expression of Obgs from bacteria and eukaryotes, many studies have focused almost exclusively on bacterial Obg homologs. As reported to date, the various *obg* mutations affect cell growth, morphological differentiation, sporulation, ribosome biogenesis, chromosome partitioning, regulation of the DNA replication and repair processes, and even stress response (Foti et al. 2005; Maddock et al. 1997; Michel 2005; Okamoto and Ochi 1998; Shepherd et al. 2002). However, even though Obgs are essential for the viability of nearly all bacteria, their primary role remains unknown.

Although the basic functions of the Obg subfamily of proteins are not clearly defined, it is noteworthy that the majority of the Obg proteins studied to date are associated with the ribosome. For example, *Bacillus* Obg was reported to coelute with ribosomal subunits and specifically interacts with the ribosomal protein L13 (Scott et al. 2000). Similarly, CgtAc, which is an Obg from *Caulobacter crescentus*, is associated with the 50S ribosomal subunit (Lin et al. 2004) and strains that carry the temperature-sensitive allele $cgtA_C$ express a reduced level of 50S subunits when compared with the wild type (Datta et al. 2004). ObgE and $CgtA_V$, which are Obgs from the gram-negative bacteria *Escherichia coli* and *Vibrio harveyi*, respectively, were also found to cofractionate with the 50S ribosomal subunit (Sikora et al. 2006; Wout et al. 2004). In addition, overexpression of *ObgE* rescued the ribosome defects of the *ΔrrmJ* strain, which is a null mutant of *rrmJ* that encodes an rRNA methyltransferase involved in late 50S ribosome assembly (Tan et al. 2002). In the *ΔrrmJ* strain, however, *ObgE* overexpression is likely not to restore the 23S rRNA modification but rather to stabilize the biogenesis of the 70S ribosome. More recently, it was reported that ObgE is involved in late steps of large-ribosome assembly (Jiang et al. 2006). Therefore, these findings raise the possibility that the Obg subfamily of GTPases play a fundamental role in the process of ribosome assembly or maturation.

Obg proteins were also described in plants (Hirano et al. 2006) (Fig. 1A), in which it was assumed that they would function as ribosome-associated GTPases essential for plant viability, similarly to what was described for bacterial Obgs. However, there have been no efforts to date to gain an insight into the roles of plant Obgs, despite the strong prediction of an importance role for these proteins in plants. In this study, we studied *Arabidopsis* AtObgC, which is a chloroplast-targeting Obg GTPase, and addressed its physiological and molecular biological properties in plants. AtObgC is a plant-specific Obg-like GTPase that comprises an N-terminal region for chloroplast targeting that is adjacent to the typical Obg structural motifs. Moreover, we found that the GFP signal of this protein exhibited a punctate staining pattern in chloroplasts, which suggested a dimerization or multimerization of AtObgC, and its Obg fold was essential for generating this pattern. We also showed that an *AtObgC* null mutation leads to an embryonic lethal phenotype, which underscores its crucial role in embryogenesis. In conclusion, our results imply that the AtObgC protein may be involved in the protein synthesis process in chloroplasts and that, consequently, its mutation affects embryogenesis severely.

Materials and methods

Database search and phylogenetic analysis

A FASTA search of the genes encoding Obg was conducted using the National Center for Biotechnology Information (NCBI) database using the amino acid sequence of *Bacillus* Obg as a query. The amino acid sequences of the Obg subfamily proteins obtained were aligned using the ClustalW software and the sequence alignment for phylogenetic analysis was performed using

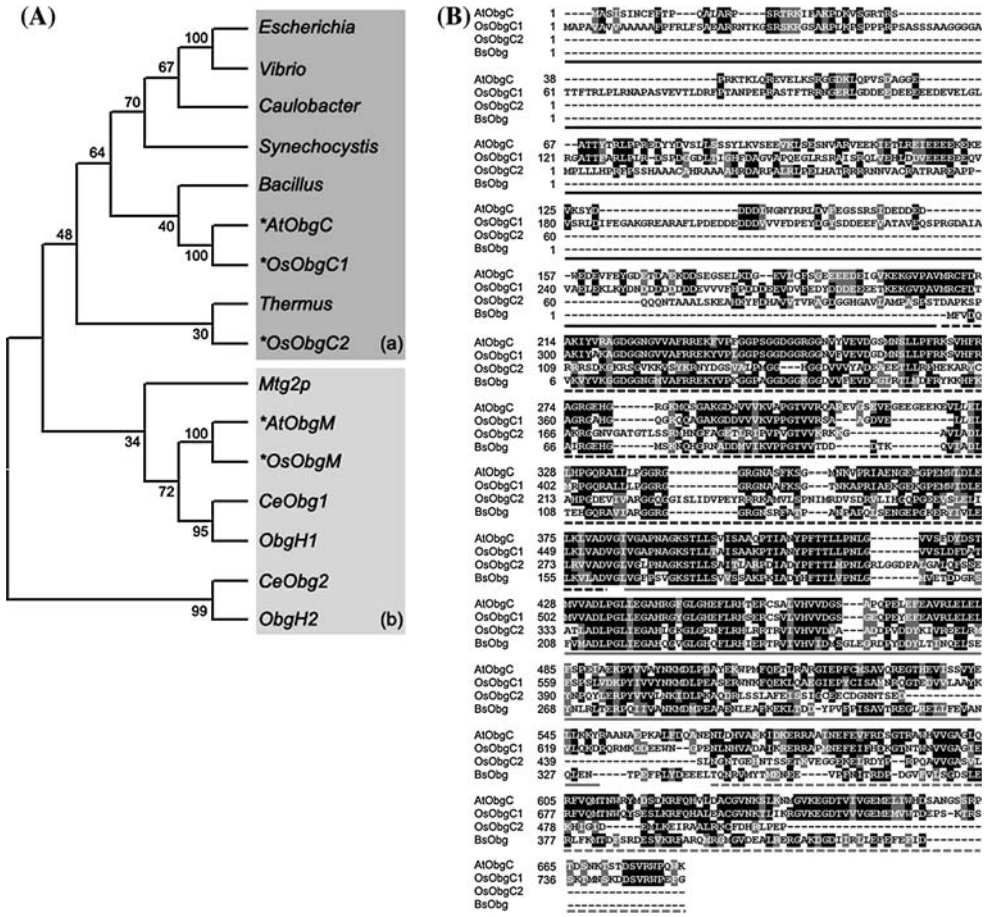

Fig. 1 Identification of Obg subfamily proteins in plants. **A** Phylogenetic tree of Obg subfamily proteins with plant Obg homologs. The phylogenetic tree was constructed using the neighbor-joining method and was tested by 100 replications of the bootstrap analysis, which was visualized using the Molecular Evolutionary Genetics Analysis (MEGA 3.1) software. Full species names and GenBank accession numbers (or Locus IDs in plants) are as follows: *Arabidopsis* (AtObgC; AT5G18570 and AtObgM; AT1G07620), *Bacillus subtilis* (NP_390670), *Caenorhabditis elegans* (CeObg1; NP_493334 and CeObg2; NP_498042), *Caulobacter crescentus* (NP_419134), *Escherichia coli* (NP_417650), *Homo sapiens* (ObgH1; NP_056481 and ObgH2; NP_001036182), *Oryza sativa* (OsObgC1; OS07G47300, OsObgC2; OS03G58540 and OsObgM; OS11G47800), *Saccharomyces cerevisiae* (Mtg2p; NP_012038), *Synechocystis* sp. (NP_440268), *Thermus thermophilus* (YP_145047), and *Vibrio harveyi* (YP_001444030). The Obg proteins were divided into two clades, i.e., bacteria (*a*) and eukaryote (*b*). The CeObg1 and CeObg2 are *C. elegans* homologs of human mitochondrial ObgH1 and nucleolar ObgH2, respectively. Mtg2p is a mitochondrial Obg from yeast. *Asterisks* indicate Obg proteins from *Arabidopsis* and rice. **B** Sequence alignments of plant-specific ObgC proteins with a bacterial Obg. Sequences include *Arabidopsis* ObgC (AtObgC), two rice ObgCs (OsObgC1 and OsObgC2), and *B. subtilis* Obg (BsObg), which was used as a typical Obg subfamily protein. Conserved Obg elements, which include the Obg fold and the GTPase and OCT domains, are shown as a *black dotted line*, a *gray line*, and a *gray dotted line*, respectively. The N-terminal region of the AtObgC and OsObgC1 proteins, which contains a putative transit peptide, is represented by a *black line*

the neighbor Molecular Evolutionary Genetics Analysis (MEGA 3.1) software (Kumar et al. 2004). The phylogenetic tree was inferred using the neighbor-joining method and was tested by 100 replications of the bootstrap analysis, which was visualized using the MEGA 3.1 software.

Materials

The *Arabidopsis* (*Arabidopsis thaliana*) plants used for protoplast preparation were grown on agar plates containing 2.1 g/l Murashige and Skoog salts and 1% sucrose. A japonica rice variety, Dongjin, was used for Northern blot analysis. The *Arabidopsis* T-DNA mutant (387B03) was generated in the context of the GABI-Kat program and was provided by Bernd Weisshaar (MPI for Plant Breeding Research, Cologne, Germany) (Rosso et al. 2003). The *AtObgC* full-length cDNA clone (U16655) was obtained from the DNA stock center of the *Arabidopsis* Biological Resource Center (ABRC) (Yamada et al. 2003). For protoplast transient assay (in Fig. 5), the *F_1-ATPase-RFP* clone as a mitochondrial marker was used (Lee et al. 2009).

Isolation of total RNA and Northern blot analysis

Total RNA was isolated from *Arabidopsis* and rice tissues using the TRI Reagent (Molecular Research Center, Cincinnati, OH), according to the manufacturer's instructions. For Northern blot analysis, 20 μg of total RNA was fractionated by electrophoresis through a 1.2% formaldehyde–agarose gel and transferred onto a nylon membrane (Schleicher & Schuell BioScience, Inc., Keene, NH), according to a standard method (Sambrook and Russell 2001). Radiolabeled probes were prepared using a random labeling kit, according to the manufacturer's instructions (Promega, San Luis Obispo, CA). After hybridization, the membranes were washed with 2 × SSC (1 × SSC: 0.15 M NaCl and 0.015 M sodium citrate) and 0.1% SDS at room temperature for 20 min followed by 0.1 × SSC and 0.1% SDS at 60°C for 30 min. Finally, the membrane was exposed to a screen and visualized using a Cyclone phosphorimager (Perkin Elmer, Foster city, CA).

GTP hydrolysis assay

The recombinant His-AtObgC$_{\Delta(1–207)}$ was expressed in *E. coli* BL21 (DE3) cells, purified via immobilized metal ion affinity purification using a Ni Sepharose 6 Fast flow column (GE Healthcare Bio-Sciences Corp, Piscataway, NJ), and eluted with imidazole. The eluted proteins were further purified by DEAE-sepharose® ion-exchange chromatography (Sigma–Aldrich, St. Louis, MO). Subsequently, the proteins were dialyzed using a buffer containing 50 mM Tris–Cl [pH 8.0], 1 mM $MgCl_2$, and 1 mM DTT, and were then subjected to GTP hydrolysis assays.

The GTP hydrolysis assays were carried out on poly(ethyleneimine)-cellulose TLC (PEI-cellulose TLC) plates, using a slight modification of a method described previously (Seo et al. 1997). Briefly, the reaction was performed in a buffer containing 20 mM Hepes [pH 7.5], 1 mM $MgSO_4$, 0.5 mM DTT, 1 mM EDTA, 1 mM NaN_3, 20 pmol of [α-^{32}P] GTP, and 1 μg of His-AtObgC$_{\Delta(1–207)}$ at 30°C. Aliquots of 10 μl were sampled at appropriate time intervals and the same volume of 0.5 M EDTA [pH 8.0] was added to stop the reaction. Samples (2 μl) were spotted onto a PEI-cellulose TLC plate, which was then developed in 0.5 M NaH_2PO_4 [pH 3.4]. After drying, the plate was exposed to a screen and was visualized using the Cyclone phosphorimager. Finally, spots were quantified using the OptiQuant software (Packard Instruments, Meriden, CT).

To measure the turnover value (k_{cat}) of His-AtObgC$_{\Delta(1–207)}$, a reaction mixture containing 1.2 μM His-AtObgC$_{\Delta(1–207)}$, 1 mM GTP, and GTPase assay buffer (20 mM Hepes [pH 7.5], 1 mM $MgSO_4$, 0.5 mM DTT, 1 mM EDTA, and 1 mM NaN_3) was incubated at 30°C for 15 h. The released phosphate was quantified using the Biomol green reagent (Biomol Research Laboratories, Plymouth Meeting, PA), according to the manufacturer's protocol.

UV crosslinking

UV crosslinking reactions were performed as described previously (Seo et al. 1997). The purified His-AtObgC$_{\Delta(1–207)}$ was incubated with 0.1 μM [α-^{32}P] GTP in 20 μl of reaction mixture (50 mM HEPES/KOH [pH 8.0], 1 mM $MgCl_2$, 1 mM EDTA, 50 mM KCl, 2 mM dithiothreitol, and 0.1% glycerol) and 40 μM of competitors (i.e., ATP, CTP, GTP, GDP, and GMP) were added for 15 min at 30°C. The mixture was irradiated on ice at a distance of 3 cm for 10 min using mineral light at a wavelength of 254 nm. After UV crosslinking, reactions were stopped by the addition of 5 μl of 5 × SDS gel-loading buffer and were separated by 10% SDS–PAGE. The gel was treated with 50 mM sodium phosphate buffer [pH 5.0] for 30 min at room temperature with low-speed shaking, stained with Coomassie Blue, destained, dried, and exposed to a screen. Finally, the film was developed using the Cyclone phosphorimager.

Complementation analysis of the obgc-t mutant with AtObgC-GFP

The fusion of the *AtObgC* and *GFP* genes was constructed as follows. First strand cDNA was synthesized from total RNA prepared from *Arabidopsis* seedlings using AMV reverse transcriptase (TaKaRa, Tokyo, Japan). The cDNA was amplified by PCR using KOD-plus-DNA polymerase (TOYOBO, Osaka, Japan), according to the manufacturer's protocol. The binary vector pBI121 was used for transformation. To obtain an AtObgC-GFP expression construct under the control of the CaMV 35S promoter, the *GUS* gene in the binary vector was replaced with the *AtObgC-GFP* fusion gene described above. The resulting construct was introduced into *Agrobcterium tumefaciens* and was used to transform the heterozygous *obgc-t* line by flower dipping (Clough and Bent 1998). Kanamycin-resistant T1 transformants were then selected and the homozygous *obgc-t* line carrying *AtObgC-GFP* was further identified by PCR analysis of the T-DNA/AtObgC junction using three kinds of primers: P1 (as a forward primer; 5′-TGAGGAAGAAGAGAAAGAAAAGGA-3′), P2 (as a reverse primer; 5′-CCCATTTGGACGTGAATGTAGACAC-3′), and P3 (as a reverse primer; 5′-GTTTATCCTATCAAAGCTTGTAACC-3′).

Transient assay using *Arabidopsis* protoplasts and GFP-fusion constructs

AtObgC inserts for the various GFP fusion constructs were prepared by PCR and the PCR products were subcloned into the pENSOTG vector, which was kindly provided by Dr. Hisashi Koiwa (Bang et al. 2006). The resulting constructs (20 μg) were introduced into 2-week-old *Arabidopsis* protoplasts by polyethylene glycol-mediated transformation, as described (Bang et al. 2008). Transformed protoplasts were incubated at 22°C in the dark. Expression of the fusion proteins was observed 2 and 3 days after transformation using an Olympus AX-70 fluorescence microscope (Olympus, Tokyo, Japan) and the images were captured with a cooled charge-coupled device camera (Olympus DP-70). The filter sets used were XF116-2 (exciter, 475AF20; dichroic, 500DRLP; emitter, 510AF23), XF33 (exciter, 535DF35; dichroic, 570DRLP; emitter, 605DF50), and XF137 (exciter, 540AF30; dichroic, 570DRLP; emitter, 585ALP) (Omega, Inc., Brattleboro, VT) for green fluorescent protein, red fluorescent protein, and Chl autofluorescence, respectively. The data were processed using the Adobe Photoshop software (Mountain View, CA).

Microscopy of mutant seeds

Seeds were removed from siliques of heterozygous *obgc-t* mutant lines at cotyledon stages of normal embryo development and were cleared in Hoyers solution (7.5 g gum arabic, 100 g chloral hydrate, 5 ml glycerol in 30 ml water), as described previously (Liu and Meinke 1998; Price et al. 1994). The fixation step was not essential, but some preparations of Hoyers were diluted to 20–30% with distilled water. Cleared seeds were examined using an Olympus BX61 microscope equipped with Nomarski optics (Olympus, Tokyo, Japan).

Results

Identification and molecular characterization of plant Obg homologs

To identify genes that encode plant homologs of the typical Obg subfamily, we performed a search of *Arabidopsis* and rice genome databases using the *Bacillus* Obg gene as a query sequence and found two *Arabidopsis* and three rice *Obg* homologs. The phylogenetic analysis of these plant Obg proteins showed that they could be divided into two groups, i.e., bacterial and eukaryotic Obg-like proteins (Fig. 1A). These proteins were further classified into chloroplast- and mitochondrion-targeting Obg proteins (based on their putative cellular localizations) using the TargetP 1.1 prediction software (http://www.cbs.dtu.dk/services/TargetP/). Accordingly, the proteins were designated as AtObgC and AtObgM in *Arabidopsis* and as OsObgC1, OsObgC2, and OsObgM in rice. Particularly, the ObgCs were much closer to bacterial Obgs than to eukaryotic Obgs, which indicates that their existence is unique to plant species among all eukaryotic organisms (Fig. 1A). Moreover, the *ObgC* genes from *Arabidopsis* and rice exhibited leaf-specific and light-inducible expression patterns (Fig. 2). Therefore, these results further support the contention that ObgC homologs may play a plant-specific role in light-dependent chloroplasts.

Here, we focused on the characterization of the plant ObgCs via the study of *Arabidopsis* ObgC. The *AtObgC* (At5g18570) cDNA was obtained from the *Arabidopsis* Information Resource (TAIR) and was sequenced to verify its integrity. *AtObgC* is predicted to encode a protein of 681 amino acids with a calculated molecular mass of about 76 kDa. The comparison of the amino acid sequences of several Obgs revealed that AtObgC in particular showed

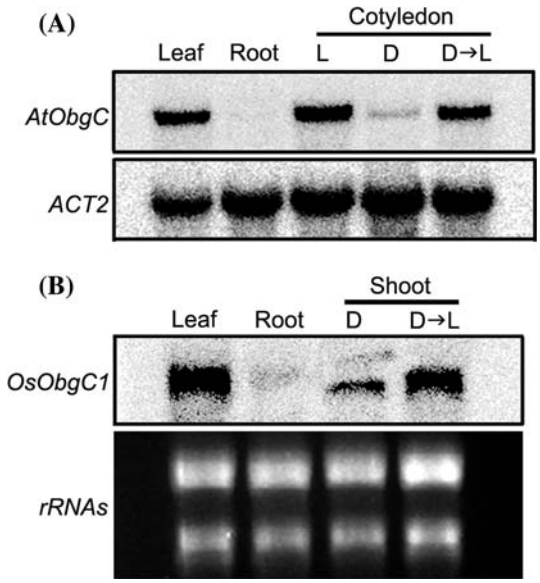

Fig. 2 Light-dependent and leaf-specific expression patterns of the *ObgC* genes. **a** Expression analysis of the *AtObgC* gene in *Arabidopsis*. Total RNA (20 μg) was prepared from juvenile leaves, roots, and etiolated cotyledons of *Arabidopsis* and was subjected to Northern blot analysis using [α-^{32}P]-labeled *AtObgC* cDNA as a probe. To assess the light-induced expression of *AtObgC* genes, the etiolated cotyledons of dark-grown seedlings were illuminated for 24 h (*D*→*L*) and the total RNA purified from these tissues was used for Northern blot analysis. The *Actin2* cDNA (*ACT2*) was used as a probe to ensure equal loading of RNA. *L* and *D* indicate light-grown and dark-grown seedlings, respectively. **b** The expression of the *OsObgC1* gene in rice was analyzed as described in (**a**). The rRNAs stained with ethidium bromide are shown as a loading control and *L* and *D* indicate light-grown and dark-grown shoots, respectively

high identity (43%) and similarity (62%) with *Bacillus* Obg (Fig. 1B). Highly conserved sequences of the Obg fold and G domain were also present in AtObgC (Fig. 1B). Although the C-terminal region of AtObgC had low similarity with that of *Bacillus* Obg, AtObgC also contained an OCT-like region in its C-terminus (Fig. 1B). However, an outstanding difference was detected between the N-terminal regions of AtObgC and *Bacillus* Obg (Fig. 1B): AtObgC contained a longer N-terminus (comprising 207 amino acids) when compared with that of bacterial Obgs. The TargetP 1.1 software predicted that this region contains a chloroplast-transit peptide composed of 32 amino acids.

AtObgC is a P-loop GTPase subjected to the typical Obg subfamily

As most Obg subfamily proteins have an intrinsic GTPase activity (Hirano et al. 2006), we examined the capacity of AtObgC to hydrolyze GTP to GDP. A preliminary test using the full-length AtObgC protein revealed its intrinsic GTPase activity (Supplemental Fig. S1 B, C). Subsequently, we purified the recombinant His-tagged AtObgC$_{\Delta(1–207)}$ (Fig. 3A) fragment of AtObgC, which corresponds to the typical Obg structure (Buglino et al. 2002; Kukimoto-Niino et al. 2004), from *E. coli* and subjected it to GTPase assays. Analysis of the GTPase activity of this protein on a PEI-cellulose/TLC plate revealed that free forms of GDP gradually increased as the incubation time progressed (Fig. 3B), which demonstrated a GTPase activity for this fragment similar to that of full-length AtObgC. This suggests that the AtObgC-specific N-terminal 207 amino acid sequence had no effect on the intrinsic GTPase activity of AtObgC. Accordingly, we used AtObgC$_{\Delta(1–207)}$ to determine its enzymatic parameter using a colorimetric assay and to compare its turnover value (k_{cat}) with those of other bacterial Obgs. The k_{cat} value of His-AtObgC$_{\Delta(1–207)}$ was 0.036 ± 0.002 min^{-1} ($n = 4$, not shown here), which was similar to those of other Obg proteins in various bacteria and human examined previously (0.014 ± 0.005 min^{-1}; 0.010 ± 0.002 min^{-1} in human; 0.038 ± 0.007 min^{-1} in *B. subtilis*; 0.017 ± 0.002 min^{-1} in *E. coli*; and 0.03 min^{-1} in *C. crescentus*) (Buglino et al. 2002; Hirano et al. 2006; Lin et al. 1999; Wout et al. 2004). Next, we also examined the ability of various nucleotides (i.e., ATP, CTP, GTP, GDP, and GMP) to compete for the binding of His-AtObgC$_{\Delta(1–207)}$ against [α-^{32}P] GTP. Both GTP and GDP were potent competitors, whereas the addition of excess amounts of ATP, CTP, and GMP had little effect on their binding to His-AtObgC$_{\Delta(1–207)}$ (Fig. 3C). These results suggest that AtObgC containing a G domain is a GTP-/GDP-binding protein and has an intrinsic GTPase activity that is comparable to that of other Obg subfamily proteins.

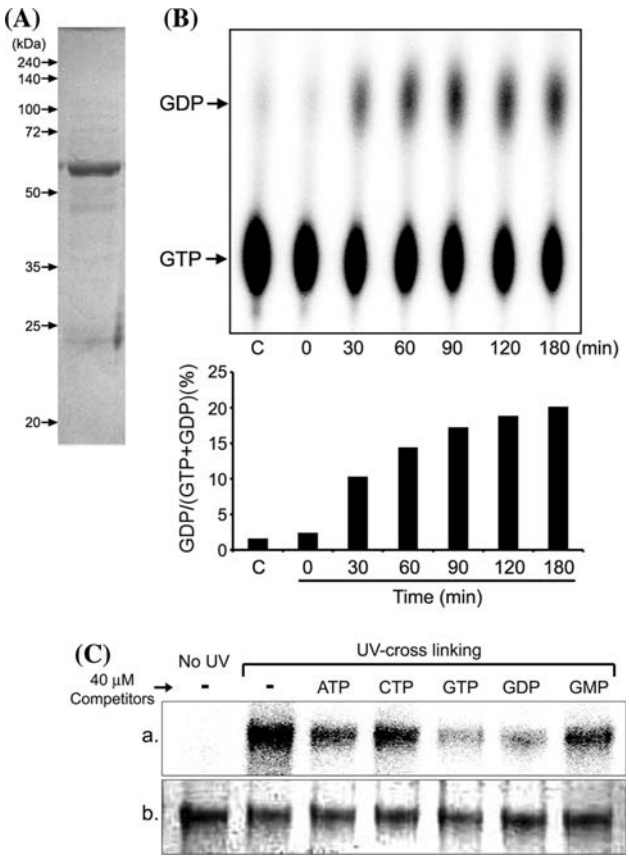

Fig. 3 GTP-binding and hydrolysis assays of AtObgC$_{\Delta(1–207)}$. **a** The 54 kDa recombinant His-AtObgC$_{\Delta(1–207)}$ protein purified from *E. coli* were analyzed on a 10% SDS–PAGE and were visualized by Coomassie blue staining. **b** Analysis of GTP hydrolysis activity. GTPase activity was measured by incubating 100 μl of reaction mixtures containing the His-AtObgC$_{\Delta(1–207)}$ protein and [α-^{32}P] GTP from 0 to 180 min. Aliquots from the reaction mixture were withdrawn, separated into GTP and GDP on a PEI-cellulose TLC plate, and visualized using a Cyclone phosphorimager (*upper panel*). *C* indicates a negative control reaction that contained no protein. To determine the GDP/(GTP + GDP) ratio (%), the relative intensities of GTP and GDP spots in the *upper panel* were measured using the OptiQuant software (*lower panel*). **c** Competition assay of the His-AtObgC$_{\Delta(1–207)}$ protein. The purified His-AtObgC$_{\Delta(1–207)}$ was incubated with [α-^{32}P] GTP in 20 μl of reaction mixture and excess amounts (400-fold) of the competing nucleotides indicated, prior to UV crosslinking. UV crosslinked AtObgC$_{\Delta(1–207)}$-[α-^{32}P] GTP complexes were visualized using the Cyclone phosphorimager (*a*) and their protein gel profiles were obtained after staining with Coomassie blue (*b*)

AtObgC localizes to chloroplasts and its transit peptide consists of more than 50 amino acid residues

Previously, within the AtObgC-specific N-terminal 207 amino acid sequence, a transit peptide composed of 32 amino acids for chloroplast targeting was predicted by the TargetP 1.1 software. Accordingly, to determine the subcellular localization of AtObgC, we generated a GFP as a cytosolic control and the *AtObgC$_{(1–207)}$-GFP* construct

(Fig. 4Aa and 4Ae, respectively). These genes were introduced into *Arabidopsis* protoplasts using the polyethylene glycol transformation method and the fluorescence of the gene products was observed by fluorescence microscopy. As shown in Fig. 4Ba and 4Be, free GFP was distributed uniformly in the cytoplasm, with the exception of chloroplasts, whereas AtObgC$_{(1–207)}$-GFP was clearly targeted to chloroplasts.

Moreover, we performed an analysis of the subcellular localization of AtObgC N-terminal truncation mutants via

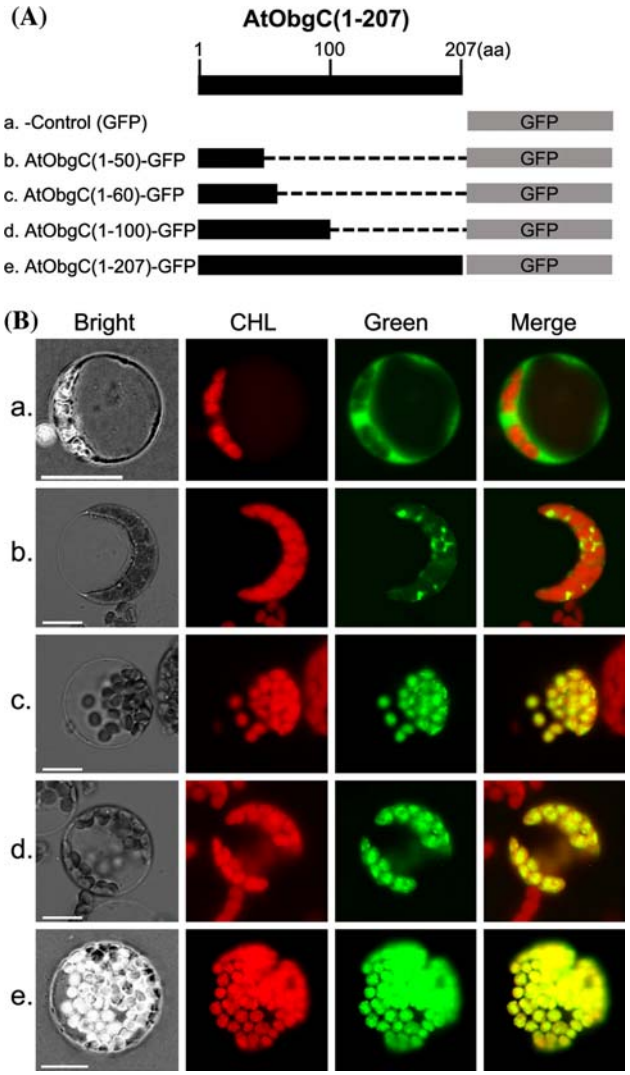

Fig. 4 Identification of a chloroplast-targeting signal peptide in AtObgC. **A** Schematic diagrams showing the four constructs used for the transient assay in protoplasts. **B** The four constructs and GFP alone (which was used as a negative control, −control) were transiently expressed in *Arabidopsis* protoplasts. The GFP signal was diffused in the cytoplasm (*a*). AtObgC$_{(1–60)}$-GFP, AtObgC$_{(1–100)}$-GFP, and AtObgC$_{(1–207)}$-GFP were targeted to the chloroplast (*c*, *d*, *e*), whereas AtObgC$_{(1–50)}$-GFP was aggregated in the cytoplasm (*b*). The *CHL* images represent chloroplasts as detected by Chl autofluorescence and were overlapped with *green* images (merge). "*Bright*" represents a bright-field image. *Scale bar* = 20 μm

transient expression of GFP-fusion proteins in *Arabidopsis* protoplasts, to dissect the chloroplast transit peptide portion of AtObgC and assess whether the targeting sequence functions properly. Three GFP-fusion constructs encoding chimeric proteins, i.e., AtObgC$_{(1–50)}$-GFP, AtObgC$_{(1–60)}$-GFP and AtObgC$_{(1–100)}$-GFP were used for the protoplast transformation, and Chl autofluorescence (CHL) was used as a control of chloroplast targeting (Fig. 4A b to d). From this assay, we found that AtObgC$_{(1–60)}$-GFP and AtObgC$_{(1–100)}$-GFP were specifically targeted to chloroplasts, whereas AtObgC$_{(1–50)}$-GFP was aggregated in the cytosol as shown in Fig. 4Bb–d. Taken together, these indicate that the AtObgC localizes to chloroplasts and its transit peptide consists of more than 50 amino acid residues.

AtObgC-GFP signal exhibits a punctate staining pattern in chloroplasts

When the GFP-fused full-length AtObgC was used for the protoplast transformation, the AtObgC-GFP exhibited a punctate staining pattern (Fig. 5 C to E), raising a question if it would localize to mitochondria. To investigate its exact distribution in either chloroplast or mitochondrium, we performed an additional experiment by using the *F_1-ATPase-RFP*, a mitochondrial marker. As shown in Fig. 5C and 5F, the green signals of AtObgC-GFP showed to be overlapped with the red ones of CHL, but it's not the case with the F_1-ATPase-RFP. Therefore, our result clearly demonstrates that the AtObgC-GFP exists in chloroplast but not in mitochondrium. Previously, ObgE was detected as a dimeric form in *E. coli* (Sato et al. 2005), and thus, it couldn't be excluded that the punctate staining pattern of AtObgC-GFP might be caused by its dimerization or multimerization.

The Obg fold, but not the G domain, is indispensable for the generation of the punctate staining pattern of AtObgC-GFP

To determine the minimal region of AtObgC necessary for the generation of the punctate staining pattern observed in chloroplasts, several AtObgC fragments were linked separately at the N-terminus of GFP to generate the chimeric proteins AtObgC$_{(1–207)}$-GFP, AtObgC$_{(1–379)}$-GFP, and AtObgC$_{\Delta(208–379)}$-GFP (Fig. 6A b–d). Subsequently, these three constructs were expressed transiently in *Arabidopsis* protoplasts and their subcellular localization was observed by fluorescence microscopy, using CHL as a positive control for chloroplast targeting. Both AtObgC$_{(1–207)}$-GFP and AtObgC$_{\Delta(208–379)}$-GFP were diffused in chloroplasts, whereas AtObgC$_{(1–379)}$-GFP exhibited a punctate staining pattern in chloroplasts, which indicates that the Obg fold (amino acid residues 208–379) of AtObgC is indispensable

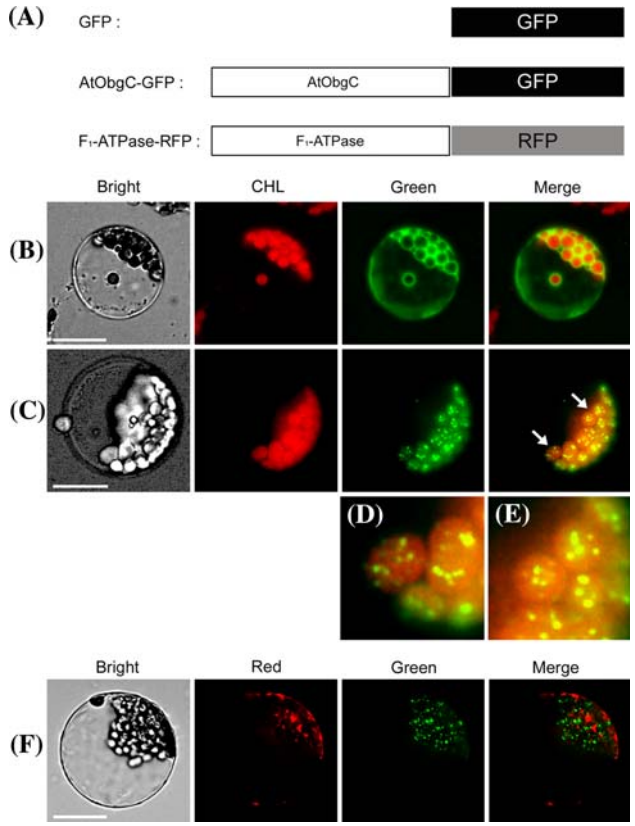

Fig. 5 Distribution of AtObgC-GFP as a punctate staining pattern in chloroplasts. **a** Schematic diagram represents the GFP-fused full-length AtObgC (AtObgC-GFP) and two negative controls such as GFP alone and F_1-ATPase-RFP as a mitochondrial marker. **b**, **c** *Arabidopsis* protoplasts isolated from 2-week-old leaves were transformed with either *GFP* (**b**) or *AtObgC-GFP* (**c**) and were observed 24 h after transformation. "*Green*" represents GFP in the transformed protoplasts. "*Merge*" shows the overlap of the GFP (*Green*) and the Chl autofluorescence (*CHL*), which was used as a marker for chloroplasts. "*Bright*" is a bright-field image. The *arrows* in the merged image of (**c**) indicate the punctate staining pattern of AtObgC-GFP, which is magnified in **d** and **e**. **f** Protoplasts were cotransformed with the *AtObgC-GFP* and *F1-ATPase-RFP*, and were observed 36 h after transformation. "*Merge*" represents the overlapped image of *Green* (AtObgC-GFP) and *Red* (F1-ATPase-RFP). *Scale bar* = 20 μm

for the generation of the punctate staining pattern (Fig. 6B b to d). A previous X-ray structural analysis of bacterial Obgs showed that their N-terminal Obg folds formed an unique architecture, which suggested a role for this domain in protein–protein interaction (Buglino et al. 2002; Kukimoto-Niino et al. 2004). Once the punctate staining pattern represents the dimerization or multimerization of AtObgC, as mentioned previously, it demonstrates that the Obg fold is crucial for such an oligomerization via the protein–protein interaction.

Moreover, since GTP binding and/or hydrolysis are required for the catalytic activity and localization of GTPases (Heo et al. 2005; Polakis and McCormick 1993), the role of the AtObgC G domain in the generation of the punctate staining pattern warranted further elucidation. Two point-mutated AtObgCs, which were generated according to the report of Okamoto et al. (1998), using *Streptomyces coelicolor* Obg, were fused independently to the N-terminus of GFP to generate the following constructs: $AtObgC_{(P387V)}$-GFP and $AtObgC_{(S392N)}$-GFP (Fig. 6A e and f). The former P387 V mutant is assumed to be defective in GTPase activity, leading to the constitutive GTP-binding form of AtObgC, whereas the latter S392 N mutant may have preferential affinity for GDP, locking the protein constitutively in GDP-binding form (Okamoto and Ochi 1998). However, transformation of these two constructs into *Arabidopsis* protoplasts revealed the same punctate staining patterns (Fig. 6B e and f), which suggest that the G domain of AtObgC is not essential for the generation of these dotted patterns in chloroplasts.

AtObgC is essential at the early stage of embryogenesis

To understand the physiological role of *AtObgC* in detail, the *Arabidopsis* T-DNA insertion mutant line (GABI-Kat line 387B03), which carries a disrupted *AtObgC* locus, was ordered from the GABI-Kat collection (Rosso et al. 2003), and its T-DNA insertion was verified by PCR analysis of the T-DNA/*AtObgC* junction. As shown in Fig. 7A and 7B, the T-DNA was inserted 692 bp downstream of the ATG start codon and the T-DNA mutant was designated as *obgc-t*. PCR analyses of the *AtObgC* locus in the mutant plants grown from GABI-Kat seeds revealed that there were no homozygous knockout plants and that only heterozygous plants were generated. The examination of the segregation ratio of the T-DNA-linked sulfadiazine resistance gene in 755 seeds of heterozygous *obgc-t* plants revealed that the number of plants resistant or sensitive to sulfadiazine were 377 and 195, respectively; however, 183 seeds failed to germinate, i.e., they were abortive (Table 1). Thus, the ratio of aborted:resistant:sensitive plants was not significantly different from the expected Mendelian segregation ratio of 1:2:1, as assessed using the chi-squared test ($\chi^2 = 0.383$, $df = 2$, $P = 0.8258$) (Table 1). Visual analysis of the silique of heterozygous *obgc-t* lines using a light microscope indicated that approximately one-quarter of the seeds exhibited a white appearance (Fig. 7C). Observation of these embryos using Nomarski optics confirmed that they were aborted at a very early stage, just before the globular stage in the embryogenesis process (Fig. 7 E and F). The aforementioned segregational and phenotypic properties of the *obgc-t* plants indicate that *AtObgC* null mutants are lethal. Furthermore, the homozygous *obgc-t* mutants, obtained after transformation of heterozygous *obgc-t* plants with the *AtObgC-GFP* construct, exhibited suppressed lethality (Fig. 7 B and G). We also verified that

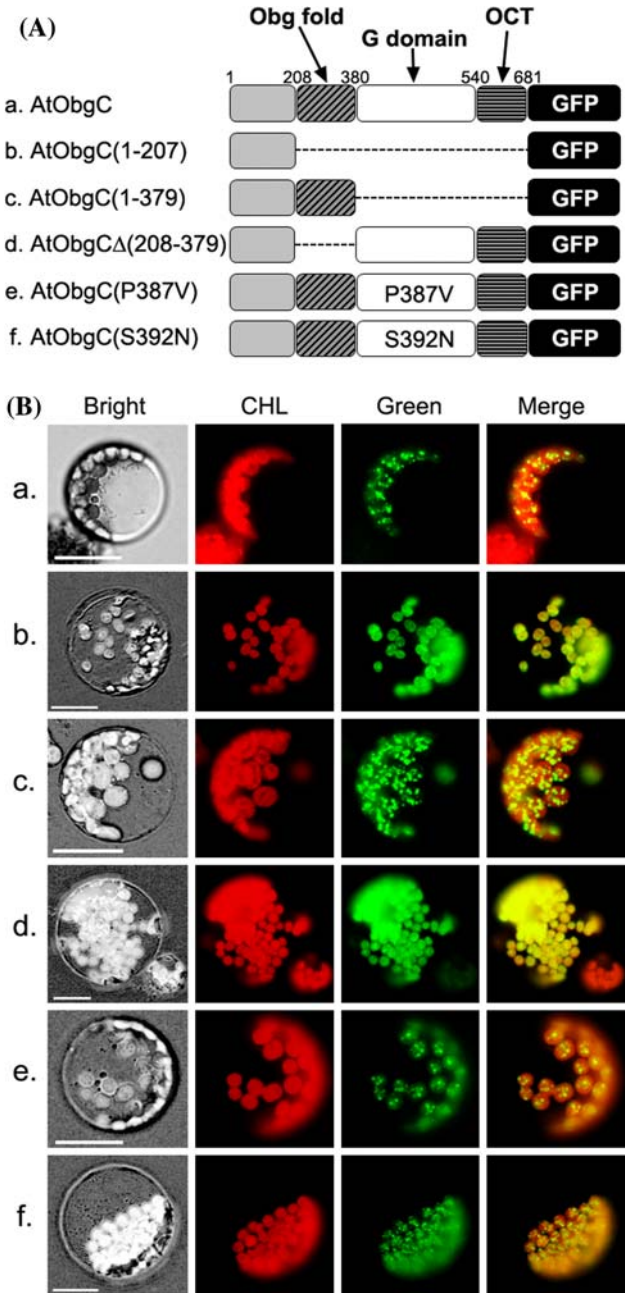

Fig. 6 Determination of the AtObgC domain necessary for the generation of the punctate staining pattern. **A** The schematic diagram represents the five AtObgC mutant constructs fused with GFP. AtObgC consists of an ObgC-unique N terminus (amino acid residues 1–207), the Obg fold (amino acid residues 208–379), the G domain (amino acid residues 380–539), and the C-terminal OCT (amino acid residues 540–681). The three deleted constructs are represented as $AtObgC_{(1–207)}$-GFP, $AtObgC_{(1–379)}$-GFP, and $AtObgC_{\Delta(208–379)}$-GFP. The remaining two GFP-fused constructs carry point mutations of AtObgC, i.e., $AtObgC_{(P387V)}$ for the GTP-binding form and $AtObgC_{(S392N)}$ for the GDP-binding form. **B** Transient assay for the definition of the region necessary for the generation of the punctate staining pattern in *Arabidopsis* protoplasts. Images show the in vivo targeting of the various GFP constructs shown in (**A**). "*Green*" represents the GFP signal in the transformed protoplasts. "*Merge*" shows the pseudocolor overlap image of "*Green*" and "CHL". *Scale bars* = 20 μm

the AtObgC-GFP exogenously expressed in the homozygous *obgc-t* mutant was targeted to chloroplasts (data not shown). These results confirmed that the lethal phenotypes observed were caused principally by the *AtObgC* locus and suggest that the disruption of the *AtObgC* gene leads to seed abortion at an early stage of embryogenesis, which demonstrates that *AtObgC* is a gene that is essential for *Arabidopsis* viability.

Discussion

Obg is a P-loop GTPase subfamily protein that is conserved in nearly all organisms from bacteria to eukaryotes and is essential for diverse biological processes in every organism in which it has been studied (Hirano et al. 2006; Michel 2005; Okamoto and Ochi 1998). Plant genomes also comprise genes that encode Obg homologs (Hirano et al. 2006). Here, we divided these into two groups, i.e., chloroplast-targeting ObgCs and mitochondrion-targeting ObgMs, according to their predicted subcellular localization (Fig. 1A). Consistently with the prediction, one of two *Arabidopsis* AtObgs was shown to be targeted to chloroplasts and was designated as AtObgC (Fig. 4 and 5), while the other AtObg localized to mitochondria and was designated as AtObgM (unpublished data). In particular, our phylogenetic analysis revealed that the ObgCs are plant-specific Obg homologs among eukaryotes (Fig. 1A) and, thus, it was suggested that ObgCs may have plant-specific functions. Here, we focused on the characterization of AtObgC, which is a chloroplast-targeting GTPase. Subsequent molecular analyses demonstrated that AtObgC is a P-loop GTPase subjected to the typical Obg subfamily and that its defect severely impaired the early stage of *Arabidopsis* embryogenesis.

Many previous studies demonstrated that the majority of bacterial Obg proteins are commonly associated with the ribosome. In detail, *Bacillus* Obg cofractionates with ribosomal subunits during gel filtration of bacterial lysates (Scott et al. 2000) and the *Caulobacter* Obg CgtAc is associated with the 50S ribosomal subunit (Lin et al. 2004). In addition, *Escherichia* ObgE and *Vibrio* $CgtA_V$ cofractionate with the 50S ribosomal subunit (Sikora et al. 2006; Wout et al. 2004). As reported to date, several mutations in bacterial *Obg* genes that encode the ribosome-associated GTPases lead to defective ribosome biogenesis. For example, strains expressing a temperature-sensitive allele of $CgtA_C$ produce a reduced level of 50S subunits when compared with the wild type (Datta et al. 2004). An *obgE* mutant exhibits ribosome profile perturbations and defects in 16S rRNA processing (Sato et al. 2005). In addition, overexpression of *ObgE* rescues the ribosome defects of the *ΔrrmJ* strain, which is a null mutant of the *rrmJ* gene

encoding the rRNA methyltransferase that is responsible for late 50S ribosome assembly (Tan et al. 2002). Although the overexpression of *ObgE* in the *ΔrrmJ* strain was not likely to restore the 23S rRNA modification, it stabilized the biogenesis of the 70S ribosome. A recent approach also revealed that ObgE is involved in the late steps of large ribosome assembly (Jiang et al. 2006). Moreover, Sato et al. (2005) reported that the ObgE had been cosedimented with rRNAs as a dimeric form after sucrose density gradient centrifugation, suggesting the involvement of rRNA processing. In this study, we proposed that the punctate staining pattern of AtObgC-GFP (Fig. 5) might represent the dimerization or multimerization of AtObgC. Furthermore, our recent preliminary work using an *AtObgC* knockdown mutant revealed that *AtObgC* was essential for plastid rRNA processing (data not shown). Taken together, these suggest that chloroplasts of higher plants originated from a cyanobacterium-like ancestor may retain the conserved roles of bacterial Obgs in ribosome biogenesis, especially in rRNA processing.

Furthermore, the phenotype of the *obgc-t* null mutant supports the hypothesis concerning the role of AtObgC in ribosome biogenesis. The homozygous *obgc-t* mutation generated by T-DNA insertion led to an embryonic lethal phenotype (Fig. 7). Similarly, lethality was found in null mutants of genes responsible for protein synthesis in chloroplasts (Berg et al. 2005; Rogalski et al. 2006; Schmitz-Linneweber and Small 2008). For example, knockout mutants of several chloroplast aminoacyl-tRNA synthetases (AARSs) exhibit an embryonic defective phenotype (Berg et al. 2005); their embryos were arrested at the globular to transition stage of development, heterozygous siliques contained about 25% of white seeds before the onset of desiccation, and the ratio of resistant to sensitive plants derived from seeds plated on selection medium was the 2:1 ratio predicted for heterozygotes with a single T-DNA insertion. These results are almost identical to our findings shown in Fig. 7 and Table 1. In addition, many null mutations of *Arabidopsis PPR* genes involved in chloroplast translation also lead to the embryonic abortion, which was

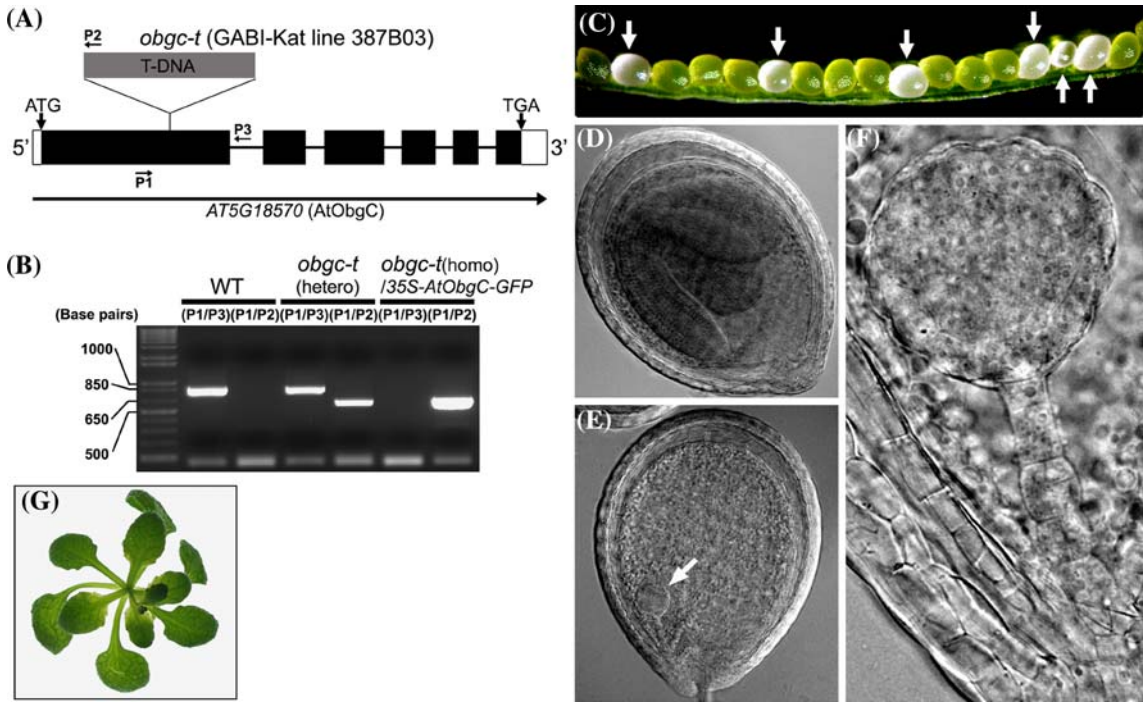

Fig. 7 Abnormal development of the *obgc-t* null mutant during embryogenesis. **a** Insertion of the T-DNA into the first exon of *AtObgC* (*AT5G18570*) locus. *Open* and *filled boxes* indicate exons encoding 5′- and 3′-UTRs and protein-coding regions, respectively. The T-DNA is shown as a *gray box*. **b** Confirmation of the T-DNA insertion at the first exon of *AtObgC*. The P1, P2, and P3 primers in (**a**) were used for PCR analysis of the T-DNA/AtObgC junction together with the genomic DNAs extracted from wild-type, heterozygous *obgc-t*, and homozygous *obgc-t*/*35S-AtObgC-GFP* plants. **c** Light micrograph of the silique of the heterozygous *obgc-t* line. *Arrows* indicate the position of representative aborted seeds (white seeds). **d–f** Morphology of embryos of a green seed and a white seed from the silique shown in (**c**) were viewed under a light microscope using Nomarski optics. Images in (**d**) and (**e**) show the embryos of green and white seeds, respectively. The *arrow* in (**e**) indicates an aborted embryo, which was further observed in the magnified image shown in (**f**). **g** Complementation analysis of the *obgc-t* mutant using the *AtObgC* gene. The image exhibits the phenotype of the homozygous *obgc-t* line containing a *35S-AtObgC-GFP* construct

Table 1 Genetic analysis of the *obgc-t* mutant

Genotype	Generation	Selection	Seeds plated on selection medium (+Sulfadiazin) Total: 755[a]		
			Aborted[b]	Resistant[c]	Sensitive[d]
obgc-t	T_3	Sulfadiazin	183	377	195
			$\chi^2 = 0.383$, $df = 2$, $P = 0.8258$[e]		

[a] 755 seeds of *obgc-t* heterozygous plants were plated on the selection medium containing sulfadiazin

[b] "Aborted" indicates seeds that did not germinate on the selection medium

[c,d] The resistant/sensitive phenotypes among the 755 seeds were scored after 21 days of growth on the selection medium

[e] Chi-squared test for the Mendelian segregation ratio of 1:2:1 (aborted: resistant: sensitive)

suggested to be caused by the failure to translate one or more of the *ycf1*, *ycf2*, and *accD* genes, which are essential for cell survival (Schmitz-Linneweber and Small 2008). Therefore, the disruption of protein synthesis in chloroplasts is likely to underlie the embryonic lethality observed in the *obgc-t* null mutant. Altogether, our results provide important clues towards the understanding of the function of AtObgC; we suggest that this molecule may be involved in the protein synthesis process in chloroplasts by taking part in ribosome biogenesis. To demonstrate this hypothesis, we are currently monitoring the specific role of AtObgC using a knockdown mutant in an attempt to circumvent the embryonic lethality.

Acknowledgments We thank Prof. Hisashi Koiwa at the Texas A&M University for the kind gift of the pENSOTG vector and Prof. Woo Sik Chung and Dr. Sang Min Lee at the Gyeongsang National University in Korea for providing the *F_1-ATPase-RFP* clone as a mitochondrial marker. J. Chen, I·S. Jeong, D.W. Kim, C·H. Im, and Y. Lee are graduate students supported by scholarships from the BK21 program at the Gyeongsang National University in Korea. This work was supported by grants from the BK21 program and the EB-NCRC (#R15-2003-012-01002-0) of the Ministry of Education and Science Technology of Korea, and by the New Energy and Industrial Technology Development Organization (the Green Biotechnology Program) and Grants-in-Aid from the Ministry of Education, Culture, Sports, Science and Technology (Nos. 18570048 and 19039030 to T.S.) of Japan.

References

Bang WY, Kim SW, Ueda A, Vikram M, Yun DJ, Bressan RA, Hasegawa PM, Bahk JD, Koiwa H (2006) *Arabidopsis* carboxyl-terminal domain phosphatase-like isoforms share common catalytic and interaction domains but have distinct in planta functions. Plant Physiol 142:586–594

Bang WY, Jeong IS, Kim DW, Im CH, Ji C, Hwang SM, Kim SW, Son YS, Jeong J, Shiina T, Bahk JD (2008) Role of *Arabidopsis* CHL27 protein for photosynthesis, chloroplast development and gene expression profiling. Plant Cell Physiol 49:1350–1363

Bar-Sagi D, Hall A (2000) Ras and Rho GTPases a family reunion. Cell 103:227–238

Berg M, Rogers R, Muralla R, Meinke D (2005) Requirement of aminoacyl-tRNA synthetases for gametogenesis and embryo development in Arabidopsis. Plant J 44:866–878

Bourne HR, Sanders DA, McCormick F (1990) The GTPase superfamily: a conserved switch for diverse cell functions. Nature 348:125–132

Bourne HR, Sanders DA, McCormick F (1991) The GTPase superfamily: conserved structure and molecular mechanism. Nature 349:117–127

Brown ED (2005) Conserved P-loop GTPases of unknown function in bacteria: an emerging and vital ensemble in bacterial physiology. Biochem Cell Biol 83:738–746

Buglino J, Shen V, Hakimian P, Lima CD (2002) Structural and biochemical analysis of the Obg GTP binding protein. Structure 10:1581–1592

Cabrera-Vera TM, Vanhauwe J, Thomas TO, Medkova M, Preininger A, Mazzoni MR, Hamm HE (2003) Insights into G protein structure, function, and regulation. Endocrine Rev 24:765–781

Caldon CE, March PE (2003) Function of the universally conserved bacterial GTPases. Curr Opin Microbiol 6:135–139

Clough SJ, Bent AF (1998) Floral dip: a simplified method for Agrobacterium-mediated transformation of *Arabidopsis thaliana*. Plant J 16:735–743

Comartin DJ, Brown ED (2006) Non-ribosomal factors in ribosome subunit assembly are emerging targets for new antibacterial drugs. Curr Opin Pharmacol 6:453–458

Czyz A, Wegrzyn G (2005) The obg subfamily of bacterial GTP-binding proteins: essential proteins of largely unknown functions that are evolutionarily conserved from bacteriato humans. Acta Biochim Pol 52:35–43

Datta K, Skidmore JM, Pu K, Maddock JR (2004) The *Caulobacter crescentus* GTPase CgtAC is required for progression through the cell cycle and for maintaining 50S ribosomal subunit levels. Mol Microbiol 54:1379–1392

Foti JJ, Schienda J, Sutera VA, Lovett ST (2005) A bacterial G protein-mediated response to replication arrest. Mol Cell 17:549–560

Heo JB, Rho HS, Kim SW, Hwang SM, Kwon HJ, Nahm MY, Bang WY, Bahk JD (2005) OsGAP1 functions as a positive regulator of OsRab11-mediated TGN to PM or vacuole trafficking. Plant Cell Physiol 46:2005–2018

Hirano Y, Ohniwa RL, Wada C, Yoshimura SH, Takeyasu K (2006) Human small G proteins, ObgH1, and ObgH2, participate in the maintenance of mitochondria and nucleolar architectures. Genes Cells 11:1295–1304

Jiang M, Datta K, Walker A, Strahler J, Bagamasbad P, Andrews PC, Maddock JR (2006) The *Escherichia coli* GTPase CgtAE is involved in late steps of large ribosome assembly. J Bacteriol 188:6757–6770

Kukimoto-Niino M, Murayama K, Inoue M, Terada T, Tame JRH, Kuramitsu S, Shirouzu M, Yokoyama S (2004) Crystal structure of the GTP-binding protein Obg from *Thermus thermophilus* HB8. J Mol Biol 337:761–770

Kumar S, Tamura K, Nei M (2004) MEGA3: integrated software for molecular evolutionary genetics analysis and sequence alignment. Brief Bioinform 5:150–163

Lee SM, Hoang MH, Han HJ, Kim HS, Lee K, Kim KE, Kim DH, Lee SY, Chung WS (2009) Pathogen inducible voltage-dependent anion channel (AtVDAC) isoforms are localized to mitochondria membrane in Arabidopsis. Mol Cells 27:321–327

Leipe DD, Wolf YI, Koonin EV, Aravind L (2002) Classification and evolution of P-loop GTPases and related ATPases. J Mol Biol 317:41–72

Lin B, Covalle KL, Maddock JR (1999) The *Caulobacter crescentus* CgtA protein displays unusual guanine nucleotide binding and exchange properties. J Bacteriol 181:5825–5832

Lin B, Thayer DA, Maddock JR (2004) The *Caulobacter crescentus* CgtAC Protein cosediments with the free 50S ribosomal subunit. J Bacteriol 186:481–489

Liu C, Meinke DW (1998) The *titan* mutants of *Arabidopsis* are disrupted in mitosis and cell cycle control during seed development. Plant J 16:21–31

Maddock J, Bhatt A, Koch M, Skidmore J (1997) Identification of an essential *Caulobacter crescentus* gene encoding a member of the Obg family of GTP-binding proteins. J Bacteriol 179:6426–6431

Michel B (2005) Obg/CtgA, a signaling protein that controls replication, translation, and morphological development? Dev Cell 8:300–301

Okamoto S, Ochi K (1998) An essential GTP-binding protein functions as a regulator for differentiation in *Streptomyces coelicolor*. Mol Microbiol 30:107–119

Polakis P, McCormick F (1993) Structural requirements for the interaction of p21ras with GAP, exchange factors, and its biological effector target. J Biol Chem 268:9157–9160

Price RA, Palmer JD, Al-Shehbaz IA, Meyerowitz EM, Somerville CR (1994) Arabidopsis. Cold Spring Harbor Laboratory Press, Cold Spring Harbor

Rogalski M, Ruf S, Bock R (2006) Tobacco plastid ribosomal protein S18 is essential for cell survival. Nucleic Acids Res 34: 4537–4545

Rosso MG, Li Y, Strizhov N, Reiss B, Dekker K, Weisshaar B (2003) An *Arabidopsis thaliana* T-DNA mutagenized population (GABI-Kat) for flanking sequence tag-based reverse genetics. Plant Mol Biol 53:247–259

Sambrook J, Russell DW (2001) Molecular cloning: a laboratory manual. Cold Spring Harbor Laboratory Press, Cold Spring Harbor

Sato A, Kobayashi G, Hayashi H, Yoshida H, Wada A, Maeda M, Hiraga S, Takeyasu K, Wada C (2005) The GTP binding protein Obg homolog ObgE is involved in ribosome maturation. Genes Cells 10:393–408

Schmitz-Linneweber C, Small I (2008) Pentatricopeptide repeat proteins: a socket set for organelle gene expression. Trends Plant Sci 13:663–670

Scott JM, Ju J, Mitchell T, Haldenwang WG (2000) The *Bacillus subtilis* GTP binding protein Obg and regulators of the σ^B stress response transcription factor cofractionate with ribosomes. J Bacteriol 182:2771–2777

Seo HS, Choi CH, Lee SY, Cho MJ, Bahk JD (1997) Biochemical characteristics of a rice (*Oryza sativa* L., IR36) G-protein a-subunit expressed in *Escherichia coli*. Biochem J 324:273–281

Shepherd PR, Salvesen G, Toker A, Graham SV, Roberts S, Buckley N, Finkel SE, Horowitz JM, Meisterernst M, Morgan I (2002) Impaired chromosome partitioning and synchronization of DNA replication initiation in an insertional mutant in the *Vibrio harveyi* cgtA gene coding for a common GTP-binding protein. Biochem J 362:579–584

Sikora AE, Zielke R, Datta K, Maddock JR (2006) The *Vibrio harveyi* GTPase CgtAV is essential and is associated with the 50S ribosomal subunit. J Bacteriol 188:1205–1210

Sprang SR (1997) G protein mechanisms: insights from structural analysis. Annu Rev Biochem 66:639–678

Tan J, Jakob U, Bardwell JCA (2002) Overexpression of two different GTPases rescues a null mutation in a heat-induced rRNA methyltransferase. J Bacteriol 184:2692–2698

Trach K, Hoch JA (1989) The *Bacillus subtilis* spo0B stage 0 sporulation operon encodes an essential GTP-binding protein. J Bacteriol 171:1362–1371

Wout P, Pu K, Sullivan SM, Reese V, Zhou S, Lin B, Maddock JR (2004) The *Escherichia coli* GTPase CgtAE cofractionates with the 50S ribosomal subunit and interacts with SpoT, a ppGpp synthetase/hydrolase. J Bacteriol 186:5249–5257

Yamada K, Lim J, Dale JM, Chen H, Shinn P, Palm CJ, Southwick AM, Wu HC, Kim C, Nguyen M (2003) Empirical analysis of transcriptional activity in the *Arabidopsis* genome. Science 302:842–846